Observation of a rotational transition in trapped and sympathetically cooled molecular ions

J. Shen, A. Borodin, M. Hansen, S. Schiller
Institut für Experimentalphysik, Heinrich-Heine-Universität Düsseldorf, 40225 Düsseldorf, Germany

We demonstrate rotational excitation of molecular ions that are sympathetically cooled by laser-cooled atomic ions to a temperature as low as ca. 10 mK. The molecular hydrogen ions HD^+ and the fundamental rotational transition $(v = 0, N = 0) \rightarrow (v' = 0, N' = 1)$ at 1.3 THz, the most fundamental dipole-allowed rotational transition of any molecule, are used as a test case. This transition is here observed for the first time directly. Rotational laser cooling was employed in order to increase the signal, and resonance-enhanced multiphoton dissociation was used as detection method. The black-body-radiation-induced rotational excitation is also observed. The extension of the method to other molecular species is briefly discussed.

I. INTRODUCTION

High-resolution laboratory rotational spectroscopy of molecules is an important and very well developed technique in molecular physics. It has provided extensive data on and insight into the structure and dynamics of molecules and has found, among other, application for the identification of molecular species in interstellar clouds. In the recent past, the accessible spectral region has been extended from the microwave region to the terahertz (THz, sub-millimeter wavelength) region, thanks to the development of appropriate THz radiation sources attaining useful power levels. Continuous-wave, narrow-linewidth THz radiation, suitable for high-resolution molecular spectroscopy, is available from backward-wave oscillators or via frequency upconversion using Schottky diodes [1, 2] or semiconductor superlattices [3, 4].

The resolution of rotational spectroscopy has been increased beyond the Doppler limit by several techniques, such as molecular beams [5], velocity-class selection [6], Lamb-dip spectroscopy, and two-photon spectroscopy [7]. For example, sub-Doppler spectral lines with widths of ca. 15 kHz around 100 GHz [8] and several 10 kHz at 0.7 - 1 THz [9, 10] have been reported. The resolution of such methods is, however, limited by transition time broadening and/or pressure broadening. In order to eventually overcome these limitations, it is interesting to explore a fundamentally different regime: trapping cold (< 1 K) molecules in an interaction-free (ultra-high-vacuum) environment and localization to sub-mm extension. Then, transition time broadening and pressure broadening, as well as Doppler broadening may be strongly reduced or even eliminated altogether. This regime may be reached with cold neutral molecules stored in optical traps or with cold molecular ions in radio-frequency traps. The production methods of cold molecules have been reviewed elsewhere, see e.g. the references [11, 12].

In this work, we take a first step towards applying high-resolution rotational spectroscopy on cold molecules: we demonstrate, for the first time to our knowledge, rotational excitation on sympathetically cooled and strongly confined molecular ions, using here temperatures as low as 10-15 mK. Our spectroscopic technique is a destructive one, resonance-enhanced multiphoton dissociation (REMPD). The particular implementation used here is 1+1'+1" REMPD, where the molecule absorbs sequentially three photons of different energy. In our work, the transitions induced by each photon corresponds to the three main energy scales of a molecule: rotational (here ca. 1 THz), vibrational (here: overtone, ca. 200 THz), and electronic (ca. 1100 THz).

With respect to the temperature of the ions and the detection method, our work is complementary of the recent demonstration of THz rotational spectroscopy of helium buffer gas cooled $H_2D^+$and D_2H^+ ions at kinetic ion temperatures of ca. 24 K, where Doppler broadening is limiting the linewidth (to ca. 1 MHz) [13].

II. THE HD^+MOLECULE AND THE SPECTROSCOPIC TECHNIQUE

The molecule we consider here, HD^+, is the most fundamental molecule with electric dipole-allowed rotational transitions [14]. Its potential as a test system for molecular quantum mechanics and for novel fundamental physics studies has been described previously [14–19]. Vibrational spectroscopy of sympathetically cooled HD^+ with the highest resolution of any molecular ion to date has recently been reported by us [20]. Pure rotational transitions have so far been observed only for the last and penultimate vibrational levels, $v = 21$, 22, close to the dissociation limit [21, 22], where their $N = 0 \rightarrow N' = 1$ transition frequencies lie in the microwave range (ca. 50 GHz and 9.4 GHz, respectively). Here we report on the rotational transition in the $v = 0$ ground vibrational level, at much higher frequency. The ro-vibrational transition frequencies have been calculated *ab-initio* with high precision [18, 19],

greatly facilitating the experimental search. The $(v = 0, N = 0) \rightarrow (v' = 0, N' = 1)$ fundamental rotational transition studied here occurs at $f_{0,th}$ = 1 314 925.752 MHz ("spinless" value, i.e. excluding hyperfine energy contributions), with an estimated theoretical error of ca. 2 kHz [23]. The $f_{0,th}$ value includes a contribution of ca. 48.8 MHz from relativistic effects (order α^2) and ca. -9.4 MHz from QED effects of order α^3.

An important aspect of this work is the use of laser rotational cooling [24], see Fig. 1. It is used to transfer most molecular population, initially distributed among several rotational levels in $v = 0$, into the ro-vibrational ground state $(v = 0, N = 0)$ and it also empties the spectroscopy target state $(v' = 0, N' = 1)$. It modifies the difference in fractional population of the lower and upper spectroscopy levels, from ca. -0.15 in thermal equilibrium to ca. 0.7, and thus significantly increases the detectable signal.

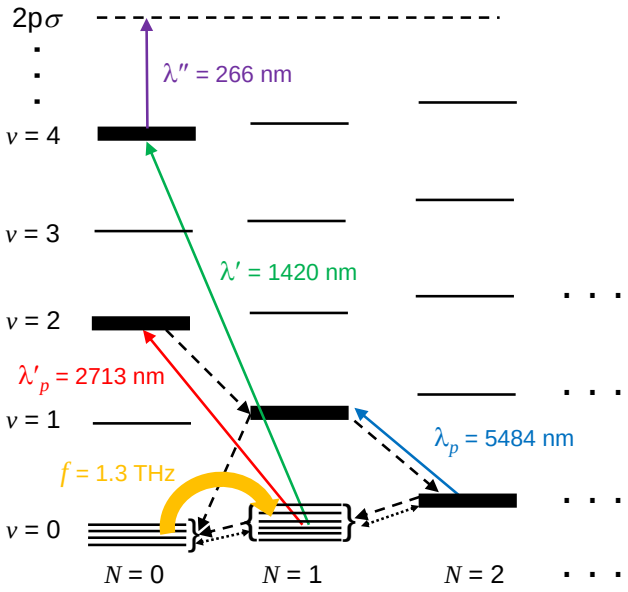

Figure 1: **Simplified energy level scheme of HD^+ with transitions relevant to this work**. Full thin arrows: laser-induced transitions, dashed arrows: some relevant spontaneous emission transitions; dotted double arrows: some relevant black-body-radiation-induced transitions. The THz wave (thick arrow) is tuned so that the four hyperfine states in $(v = 0, N = 0)$ are excited to corresponding hyperfine states in $(v' = 0, N' = 1)$. Resonant laser radiation at λ' (1420 nm) and non-resonant radiation at λ'' (266 nm) transfer the rotationally excited molecules to a vibrationally excited level $(v'' = 4, N'' = 0)$ and then further to electronically excited molecular states (predominantly $2p\sigma$), from which they dissociate. Rotational cooling is performed by radiation at λ_p (5.5 µm) and λ'_p (2.7 µm). The level energy differences are not to scale. Hyperfine structure is indicated very schematically for the levels $(v = 0, N = 0, 1)$ and as thick lines for some other participating levels. The waves at λ', λ'', λ_p, λ'_p have relatively large spectral linewidths.

The hyperfine structure and the Zeeman effect of the lower and upper ro-vibrational levels are important aspects in the rotational spectroscopy [25, 26]. As Fig. 2 shows, the ground state possesses four hyperfine states and altogether 12 magnetic substates (with magnetic quantum number J_z). In the ions' region the magnetic field is nonzero, lifting the magnetic degeneracy, The spectrum contains a large number of transitions with relatively large transition dipole moments, see Fig. 3. Most transitions, even the $\Delta J_z = 0$ ones, shift by on the order of 100 kHz or more in a field of strength 1 G. Exceptions include five (strong) $J_z = 0 \rightarrow J'_z = 0$ transitions, whose quadratic Zeeman shifts in 1 G are at most 6.2 kHz in absolute value [26]. From each lower hyperfine state there is at least one such transition; the state $(F = 0, S = 1, J = 1, J_z = 0)$ has two. Three of them are indicated by the first, third, and fourth arrow (from the top) in Fig. 2. A fourth is the hyperfine transition $(F = 1, S = 1, J = 1, J_z = 0) \rightarrow (F' = 1, S' = 1, J' = 2, J'_z = 0)$. Its transition frequency $f = f_{0,th} + 11.78$ MHz is close to other transition frequencies and is therefore not considered suitable for the present work. Instead, we use the $(F = 1, S = 1, J = 1, J_z = 0) \rightarrow (F' = 1, S' = 1, J' = 0, J'_z = 0)$. transition (second arrow in Fig. 2), which, however, exhibits a much larger quadratic Zeeman effect, e.g. 78 kHz at 1 G. The magnetic field in the trap region is not spatially constant in direction and magnitude, so some line broadening can be expected.

The theoretical Doppler linewidth is ca. 55 - 70 kHz for the lowest temperatures used here (10 - 15 mK) and ca. 150 - 200 kHz if the ion ensemble is in the liquid state (100 - 200 mK). Note that the values are relatively large due to the low mass of the HD^+ ion. At 10 - 15 mK the molecular ions are well confined along the axis of the trap and

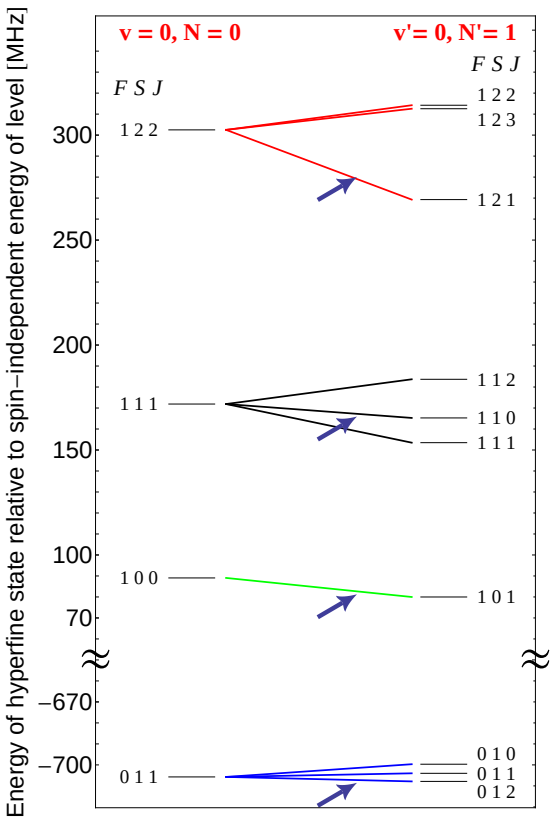

Figure 2: **Energy diagram of the hyperfine states and main electric-dipole transitions in zero magnetic field.** Left side: ro-vibrational ground level ($v = 0$, $N = 0$), right side: rotationally excited level ($v' = 0$, $N' = 1$). The hyperfine states are labeled by the (in part approximate) quantum numbers (F, S, J). The degeneracy factor of each hyperfine state is $(2J + 1)$. Transitions that do not change the quantum numbers F, S are relatively strong and are indicated by red, black, green, and blue lines. The four transitions addressed simultaneously in this work are indicated by arrows.

their motion in transverse direction is restricted to a range smaller than the THz wavelength (0.23 mm). In the axial direction, the confinement is not as strong, since diffusive motion of the ions is still occurring along the crystal axis, which exceeds in length (ca. 1.5 mm) the THz wavelength. Thus, Doppler broadening may still be present in our experiment, even at the lowest temperatures. The THz source has a linewidth below 100 Hz and sub-Hz absolute frequency stability, values that are not relevant in comparison to other line broadening effects.

The Doppler linewidth is smaller than the typical spacing between hyperfine transitions originating from different ground hyperfine states, even in presence of a magnetic field on the order of 1 G. This is in principle advantageous, since it could permit to resolve the hyperfine structure. However, detecting individual hyperfine lines would also lead to a small signal-to-noise ratio: the individual hyperfine levels each contain only a fraction of the total population. If a statistical population distribution were produced by action of the black-body radiation field (BBR) and of the rotational cooling lasers, each substate would contain 1/12 of the total population, this fraction being typically 30 molecules. The individual populations are likely to vary significantly in time, requiring the collection of substantial data and averaging. We do not attempt to do so here and in order to obtain a sufficiently strong rotational excitation signal we have applied the following strategy.

We irradiate the molecules sequentially on THz frequencies corresponding to strong hyperfine transitions. Different frequency sets are used, see Table I. Each frequency from a set is irradiated for 200 ms, and is meanwhile frequency-modulated by ± 2 kHz at a 5 Hz rate. The list is repeated several times for a total of 3 s or more, depending of the excitation approach used.

The frequency lists include three of the five above mentioned low-Zeeman-shift $J_z = 0 \rightarrow J'_z = 0$ transitions, which originate from three of the four hyperfine states of ($v = 0$, $N = 0$), and the respective frequency values have been chosen to be those corresponding to an assumed magnetic field of 1 G. As mentioned above, the chosen transition starting from the fourth hyperfine state, ($F = 1$, $S = 1$, $J = 1$) has a substantial quadratic Zeeman effect. We

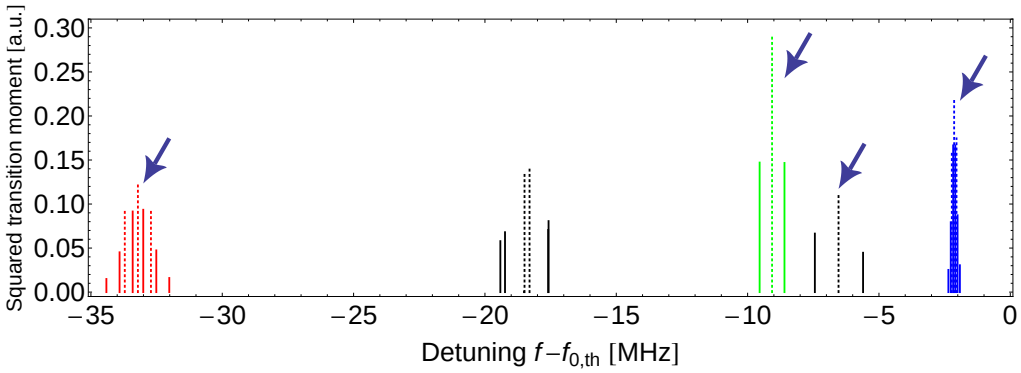

Figure 3: **Section of the theoretical stick spectrum of the rotational transition in the frequency range relevant to this work, showing the Zeeman splittings and shifts in a 1 G magnetic field.** Dashed lines are π transitions, full lines are σ transitions. $f_{0,th}$ is the theoretical "spinless" transition frequency. The four THz frequencies of list A (see Table I) are indicated by the arrows. The colors used correspond to those used in Fig. 2.

Lower hyperfine level (F, S, J)	(1,2,2)	(1,1,1)				(1,0,0)	(0,1,1)
	Frequency $f_i - f_{0,th}$ [MHz]						
List A'	-33.211	-6.597	-6.578	-6.558	-6.539	-9.069	-2.138
List A	-33.211	-6.539				-9.069	-2.138
List B	-34.993	-7.850				-9.773	-2.465
List C	-31.408	-5.096				-8.355	-1.812
List D	-34.102	-7.194				-9.421	-2.301
List E	-32.310	-5.817				-8.712	-1.975
"500 MHz detuning"	500						

Table I: **Frequency lists used for excitation of the rotational transition.** f_i is the THz frequency.

therefore attempt to compensate for the lack of precise knowledge of the magnetic field by exciting at four distinct frequencies, corresponding to the shifts induced by the magnetic field values (0.25, 0.5, 0.75, 1) G (the detuning for 0 G is -6.617 MHz). Altogether, this list of frequencies (denoted by A', see Table I) should nominally excite four of the twelve Zeeman substates. However, in the presence of a significant Doppler broadening, more substates (with larger Zeeman shifts) will be addressed. Indeed, the frequencies necessary to excite all Zeeman substates of the ground hyperfine states fall into ranges of ca. $(\pm 0.5\,,\,(\pm 1\,),\,-\,,\,\pm 0.22)$ MHz at 1 G, relative to the frequencies of the list A'. These spreads have a partial overlap with the Doppler broadening at the higher molecular temperatures (100 - 200 mK) employed here.

In order to obtain information about the detuning dependence of the rotational excitation, we also apply "detuned-frequency lists". Lists labeled B and C are detuned to smaller and larger frequencies, respectively, relative to list A' (detunings of list B: $(-1.782, -1.311, -0.704, -0.327)$ MHz, detunings of list C: (1.803, 1.443, 0.714, 0.326) MHz). The detunings are larger than the shift induced by the Zeeman effect in a 1 G field.

Lists D, E have detunings approximately half as large as those of lists B, C, respectively (list D: $(-0.891, -0.655, -0.352, -0.163)$ MHz and list E: (0.901, 0.722, 0.357, 0.163) MHz).

Finally, a list A is also used, which is a simplified version of list A'.

Frequency modulation is used in all cases.

III. EXPERIMENTAL APPARATUS AND PROCEDURE

A schematic of our apparatus [27] is shown in Fig. 4. The UHV chamber houses a linear ion trap driven at 14.2 MHz. HD gas is loaded into the chamber by opening a piezoelectric valve, after which it is ionized by an electron gun. The laser radiation for REMPD enters from the left, the 313 nm cooling radiation [28] from the right. The rotational cooling radiation enters diagonally. The THz source is positioned close to the vacuum chamber and its wave is focused into the chamber center by a concave paraboloidal mirror oriented at right angle to the beam. With a manual flip mirror, the wave can be sent to a Golay cell detector for power monitoring purposes. The THz source

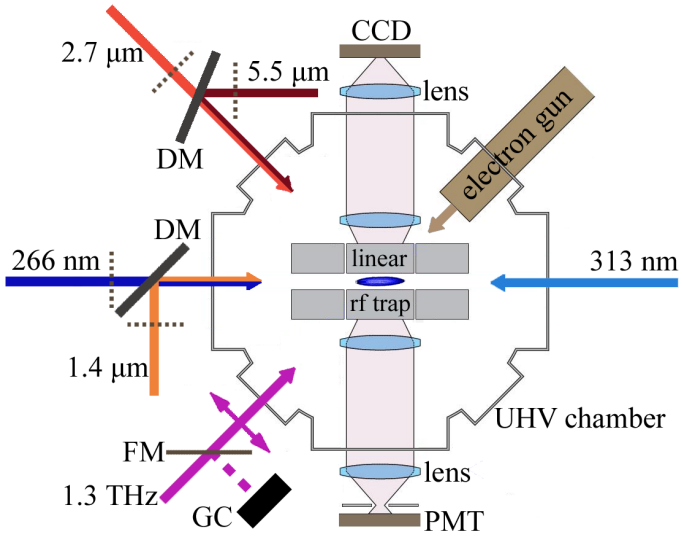

Figure 4: **Schematic of the apparatus and beams.** GC: Golay cell; FM: flip mirror; DM: dichroic mirror; dotted lines: electrically controlled laser beam shutters. The double arrow indicates the polarization of the THz wave. Not to scale.

has been described previously [29]. It is driven at the 72^{nd} subharmonic of the desired frequency, near 18 GHz. This signal is provided by a microwave synthesizer, which is frequency-locked to a to a GPS-referenced hydrogen maser. The first REMPD laser is a diode laser emitting at the wavelength $\lambda = 1420\,\text{nm}$ and exciting the $(v = 0,\, N = 1) \rightarrow (v' = 4,\, N' = 0)$ transition. The second REMPD laser excitation is non-resonant and is provided by a resonantly frequency-doubled 532 nm laser. Initially, a Be^+ ion crystal is produced in the trap. Typically, the same Be^+ ion crystal is used for several hours of experimentation.

The molecular sample preparation routine starts by frequency-stabilization of the cooling laser to a frequency a few tens of MHz to the red of the frequency for optimal Be^+ cooling, using a hyperfine transition of molecular iodine as reference. Then, a small amount of HD gas is let into the chamber and ionized by the electron gun. Both HD^+ ions as well as heavy impurity ions are generated, trapped and quickly sympathetically cooled. In order to remove these impurity ions, the dc quadrupole potential is briefly increased, reducing the quasi-potential strength in one transverse direction. The heavy ions then escape from the trapping region. This ends the preparation procedure; the produced cold HD^+ sample contains typically ca. 300 molecules.

The acquisition of one data point proceeds as follows: (i) the THz excitation is initially effectively kept off by detuning the frequency by 500 MHz from the rotational resonance, and the REMPD lasers are off as well; (ii) the rotational cooling laser beams are unblocked, and a repeated secular frequency scan (740 - 900 kHz) is activated and kept on during the remainder of the measurement cycle (method I). The heating of the molecular ions heats the Be^+ ions sympathetically and spectrally broadens their 313 nm absorption line. This leads to a substantial increase of the cooling-laser stimulated atomic fluorescence, due to the laser's relatively large detuning from atomic resonance. The

fluorescence signal level is indicative of the initial number of HD^+ in the ion ensemble. (iii) For a duration $T_c = 35\,\mathrm{s}$ the rotational cooling takes place, after which the 2.7 µm rotational cooling laser is blocked (not the 5.5 µm laser), (iv) the REMPD lasers are unblocked and simultaneously the THz frequency scan is initiated. The resulting molecule loss reduces the heating and thus the atomic fluorescence signal. (v) The change in fluorescence as a function of time is followed until the signal essentially reaches the level in absence of molecules. (Fig. 5 displays the first 60 s only). The secular excitation is kept on all the time. This concludes acquisition of one data point.

In an alternative measurement mode (method II), the secular scan activated in step (ii) to obtain a normalization signal is turned off after a few seconds while the rotational cooling continues. At the end of step (iii) both rotational cooling lasers are blocked. In step (iv), the THz source and the REMPD lasers are turned on only for 3 s. Immediately afterward, in step (v) the secular excitation is turned on again and the reduced fluorescence level is recorded during a few seconds. The ratio of the two fluorescence levels defines our signal, and gives approximately the relative decrease in HD^+ number after REMPD.

At the end of either procedure, residual HD^+ and product ions are removed from the trap by applying the following cleaning procedure. (In method II, we do not "re-use" the remaining molecules as we prefer to excite molecular samples prepared in the same way each time.) The cooling laser is detuned by a few 100 MHz to the red of the atomic cooling transition, causing melting of the crystal into a liquid. A secular excitation frequency scan covering the frequencies of HD^+ and lighter ions is turned on. The cooling laser is briefly blocked and unblocked several times. Light ions are thereby ejected from the trap. The secular excitation is turned off and the system is ready for a new molecule loading.

IV. RESULTS AND DISCUSSION

The first set of measurements was taken in the liquid state and using method I. Figure 5 shows two atomic fluorescence traces. The upper (black, "background") trace was obtained with the THz wave frequency detuned by 500 MHz from $f_{0,th}$, a value where no transition line exists. The REMPD only dissociates molecules in the ($v = 0$, $N = 1$) level. This level has initially been depopulated by the 2.7 µm rotational cooling laser, which is favorable for the purpose of the spectroscopy. But as soon as the spectroscopy phase starts, the level receives population not only by THz rotational excitation (if the frequency is near resonance), but also by BBR induced excitation from all hyperfine states of the ground ro-vibrational level (rate ca. 0.09/s). In addition, population still present in the ($v = 0$, $N = 2$) level or reaching it from higher-lying rotational levels is transferred into ($v = 0$, $N = 1$) by BBR-stimulated emission (rate ca. 0.12/s) and spontaneous emission (rate ca. 0.06/s). Therefore, a REMPD-induced molecule loss is always present.

A rate equation simulation yields a molecule number decay rate that depends on REMPD laser intensities and reaches ca. 0.075/s in the limit of very high intensities. After partial optimization of the UV laser alignment onto the ion crystal and therefore maximization of its intensity, we observed values of ca. 0.04/s at 25 s after REMPD laser turn-on. The value of the rate at this time rather than at 0 s is considered since at 0 s the number of molecules present is larger and this may lead to some saturation of the secular excitation signal. We explain the difference compared to the theoretical maximum by the actually available laser power and possibly imperfect REMPD laser beam overlap.

The lower (blue) trace represents the decay in presence of resonant THz radiation, using frequency list A'. We observe a large difference in the initial rate of signal decrease as compared to the background trace. Note that the decay occurring in presence of resonant THz radiation also contains the background decay.

We also performed measurements with the two frequency lists B, C, for which the frequencies were detuned from those of list A' by different amounts for the four hyperfine states. As Fig. 6 shows, the decay rates do not differ significantly from the background decay rates, and we can therefore deduce an upper limit for the magnetic field of 1.5 G, as the influence of the Doppler width is not significant here.

A second set of measurements was taken with method II, see Fig. 6. Here, the THz radiation is applied only when the ion ensemble is well-crystallized, at temperatures of ca. 10 - 15 mK. Data points were taken alternately at 500 MHz detuning, with list A, with list B (D), and with list C (E). Again, a finite (background) signal is observed when the THz radiation is far detuned, since BBR excites the rotational transition significantly on the used timescale of 3 s. Irradiation with the frequency list A provides a clear signal that rotational excitation induced by THz radiation takes place. We find again no significant difference in the rotational excitation efficiency for the detunings of lists B and C, compared to the background measurement. However, reducing the detunings to half the values (lists D, E), shows an increase of signal. This increase can be explained by the presence of a magnetic field of ca. 1 G or a Doppler width of several 100 kHz, or a combination of both. However, the Doppler width is at most 70 kHz under the operating conditions, therefore we conclude that we observed the effect of the magnetic field on the hyperfine transition frequencies

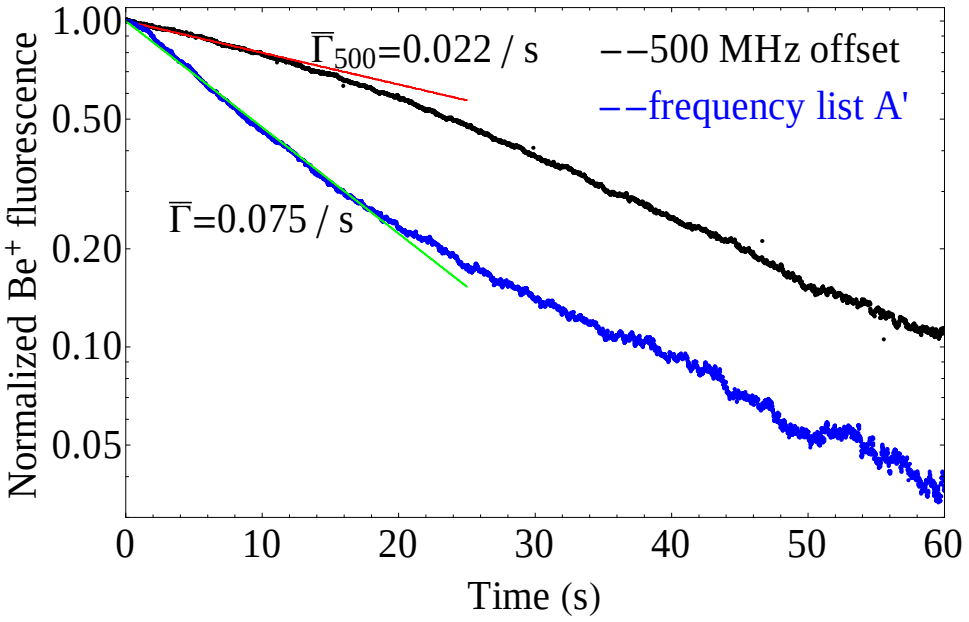

Figure 5: **Atomic fluorescence signal during continuous secular excitation of the HD^+ions (method I, liquid state).** The time axis starts after the 2.7 µm rotational cooling laser is turned off and the two REMPD lasers and THz radiation are turned on. The upper (black) trace, where the THz radiation is detuned from resonance, shows the molecular ion number decay due mainly to the effect of black-body-radiation-induced rotational excitation. Lower (blue) trace: THz radiation is on-resonance. Each trace is the average of 10 individual decays. The lines are exponential fits to the first 10 s of the data.

V. CONCLUSION

We observed, for the first time, a pure rotational excitation of a sympathetically cooled molecular ion ensemble. In order to facilitate the observation, we applied a scheme adapted to the particularities of the apparatus. As the available detection scheme is a destructive one that employs photodissociation of the rotationally excited molecules, a new molecular ion loading cycle has to be implemented for each data point and the data acquisition rate is very low. The number of ions sympathetically cooled is also small. Therefore, the preparation of a significant fraction (ca. 70%) of the molecular ions in the lower spectroscopic level was essential. Even so, the detection of a rotational transition originating from a single hyperfine state has too low a signal-to-noise ratio. This is due to the concurrent process of black-body-radiation-induced rotational excitation, which yields a finite background signal (decay rate) in connection with the photodissociation.

We therefore applied THz radiation at four frequencies that nominally excite the four hyperfine states in the lower spectroscopic level. This allowed a clear observation of the rotational excitation, using two different methods. By applying THz radiation detuned from the nominal resonance frequencies by amounts varying from 0.16 to 0.9 MHz for the four frequencies, we found a significantly reduced, but still observable excitation. This can be explained by the presence of a magnetic field with values up to approximately 1 G. In comparison, the contribution of ion motion to the linewidth when the ions are at ca. 10 mK and well-confined is negligible.

There is a strong motivation for further development of the method demonstrated here, since a resolution of the hyperfine structure of $HD^+$and an accurate measurement of the hyperfine transition frequencies would represent a significant test of the *ab-initio* calculations of this molecule. Possible improvements are the application of hyperfine state preparation techniques, recently demonstrated [20], and accurate control of the magnetic field in the trap region.

Finally, it is useful to consider the extension of this work to other molecular species. These can be characterized by their mass and their rotational constant, which are to a certain extent related. For many species, the masses will be significantly larger and the rotational constants significantly smaller than in the case of HD^+. The smaller rotational constant will lead to a significantly smaller transition frequency, in the microwave regime. It is likely that the Lamb-Dicke regime will then be effective, in particular if the microwave propagation direction is along the narrow width of the molecular ion ensemble, and Doppler broadening would be absent altogether. The smaller rotational constant will also lead to a smaller black-body-radiation excitation rate (at 300 K), which is very favorable, since

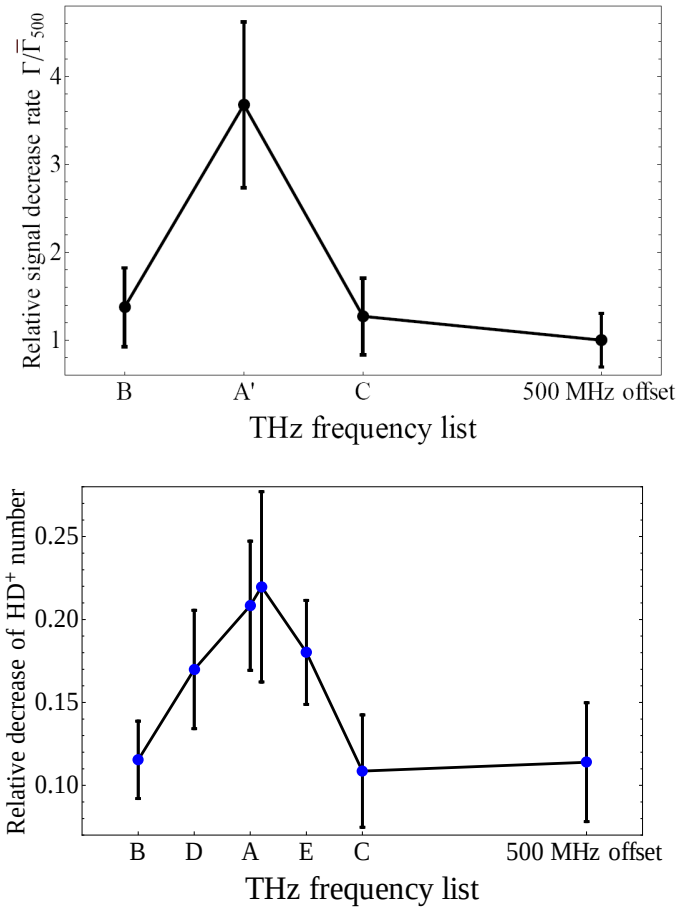

Figure 6: **Frequency dependence of the rotational excitation.** Top: in the liquid state, at ca. 100 - 200 mK, using method I. $\bar{\Gamma}_{500}$ is the average decay rate when the THz radiation frequency is detuned by 500 MHz. Each data point results from 9 individual decays.
Bottom: in the crystallized state, at 10 - 15 mK, using method II. Each data point represents the mean of 9 or 10 measurements. The two close points were taken with the same list A on different days and are shown separated for clarity. The error bars in both plots show the standard deviations of the data, not of the mean. The lines are guides for the eye.

it will make possible REMPD with near-zero background. The experimentally demonstrated fraction of molecules in the ground state obtained by applying rotational cooling on such heavier molecules is so far significantly below the level used here on HD^+[30], but simulations [31] show that similar levels should be achievable with appropriate laser cooling schemes and laser systems. Hyperfine structure and Zeeman shifts coefficients will be molecule-specific. Molecular ions in an electronic spin singlet state are particularly interesting, as they would have a reduced number of hyperfine states, Zeeman sub-states and much reduced linear Zeeman shift coefficients, simplifying and narrowing the spectrum. Thus, the extension of rotational spectroscopy of sympathetically cooled molecular ions to other species appears very promising.

Note added: With an improved alignment of the UV laser, an increase of the decay rate in absence of THz radiation to ca. 0.060/s was observed.

Acknowledgment

This work was funded by the DFG (project Schi 431/11-1) and by an equipment grant of the Heinrich-Heine-Universität. We thank F. Lewen for loan of equipment and V. Korobov for communication of unpublished results.

We are indebted to B. Roth and T. Schneider for their contributions in the initial phase of this study.

[1] F. Lewen, S. P. Belov, F. Maiwald, T. Klaus, G. Winnewisser, "A quasi-optical multiplier for terahertz spectroscopy", Z. Naturforsch. **50** a, 1182-1186 (1995)

[2] A. Maestrini, J. Ward, G. Chattopadhyay, E. Schlecht, I. Mehdi, "Terahertz sources based on frequency multiplication and their applications", Frequenz - J. of RF-Engineering **62**, 118-122 (2008).

[3] F. Klappenberger, K.F. Renk, P. Renk, B. Rieder, Y.I. Koshurinov, D.G. Pavelev, V. Ustinov, A. Zhukov, N. Maleev, A. Vasilyev, "Semiconductor-superlattice frequency multiplier for generation of submillimeter waves", Appl. Phys. Lett. **84**, 3924-3926 (2004)

[4] C. P. Endres, F. Lewen, T. F. Giesen, S. Schlemmer, D. G. Paveliev, Y. I. Koschurinov, V. M. Ustinov, and A. E. Zhucov, "Application of superlattice multipliers for high-resolution terahertz spectroscopy", Rev. Sci. Instr. **78**, 043106 (2007); DOI: 10.1063/1.2722401

[5] see e.g. H.W. Kroto, *Molecular Rotation Spectra* (Wiley, 1975)

[6] S. Carocci, A. Di Lieto, A. Menciassi, P. Minguzzi, and M. Tonelli, "High-resolution rotational spectroscopy of CH_3I using a novel Doppler-free technique", J. Molec. Spectr. **175**, 62–67 (1996)

[7] L. A. Surin, B. S. Dumesh, F. S. Rusin, G. Winnewisser, and I. Pak, "Doppler-free two-photon millimeter wave transitions in OCS and CHF_3", Phys. Rev. Lett. **86**, 2002-2005 (2001)

[8] G. Cazzoli, L. Dore, C. Puzzarini and S. Beninati, "Millimeter- and submillimeter-wave spectrum of $C^{17}O$. Rotational hyperfine structure analyzed using the Lamb-dip technique ", Phys. Chem. Chem. Phys. **4**, 3575–3577 (2002); DOI: 10.1039/b203245g

[9] G. Winnewisser, S. P. Belov, Th. Klaus, and R. Schieder, "Sub-Doppler measurements on the rotational transitions of carbon monoxide", J. Molec. Spectr. **184**, 468–472 (1997)

[10] V. Ahrens, F. Lewen, S. Takano, G. Winnewisser, S. Urbana, A. A. Negirev, and A. N. Koroliev, "Sub-Doppler saturation spectroscopy of HCN up to 1 THz and detection of J = 3 → 2 (4 → 3) Emission from TMC1", Z. Naturforsch. **57** a, 669–681 (2002)

[11] R. Krems, B. Friedrich, W.C. Stwalley, eds., *Cold Molecules* (CRC Press, 2009)

[12] I.W.M. Smith, ed., *Low Temperatures and Cold Molecules* (World Scientific Publishing, 2008)

[13] O. Asvany, O. Ricken, H. S. P. Müller, M. C. Wiedner, T. F. Giesen, and S. Schlemmer, "High-resolution rotational spectroscopy in a cold ion trap: H_2D^+ and D_2H^+", Phys. Rev. Lett. **100**, 233004 (2008); doi: 10.1103/PhysRevLett.100.233004

[14] W.H. Wing, G. A. Ruff, W.E. Lamb, J.J. Spezeski, "Observation of the infrared spectrum of the hydrogen molecular ion HD^+", Phys. Rev. Lett. **36**, 1488 - 1491 (1976)

[15] A. Carrington, I.R. McNab, and C.A. Montgomerie, "Spectroscopy of the hydrogen molecular ion", J. Phys. B: At. Mol. Opt. Phys. 22, 3551 (1989); doi:10.1088/0953-4075/22/22/006

[16] J.C.J. Koelemeij, B. Roth, A. Wicht, I. Ernsting and S. Schiller, "Vibrational spectroscopy of HD^+ with 2-ppb accuracy", Phys. Rev. Lett. **98**, 173002-4 (2007); doi:10.1103/PhysRevLett.98.173002

[17] S. Schiller and V. Korobov, "Tests of time-independence of the electron and nuclear masses with ultracold molecules", Phys. Rev. A **71**, 032505 (2005); doi:10.1103/PhysRevA.71.032505

[18] V.I. Korobov, "Leading-order relativistic and radiative corrections to the rovibrational spectrum of H_2^+ and HD^+ molecular ions", Phys. Rev. A **74**, 052506 (2006); doi:10.1103/PhysRevA.74.052506

[19] V.I. Korobov, "Relativistic corrections of $m\alpha^6$ order to the ro-vibrational spectrum of H_2^+ and HD^+ molecular ions", Phys. Rev. A **77,** 022509-11 (2008); doi: 10.1103/PhysRevA.77.022509

[20] U. Bressel et al., submitted to Phys. Rev. Lett. (2011)

[21] A. Carrington, C. A. Leach, A. J. Marr, R. E. Moss, C. H. Pyne, and T. C. Steimle, "Microwave spectra of the D_2^+ and HD^+ ions near their dissociation limits ", J. Chem. Phys. **98**, 5290 (1993); doi:10.1063/1.464928

[22] A. Carrington, I. R. McNab, C.A. Montgomerie, J. M. Brown, "Microwave spectra of the HD and D_2 ions at their dissociation limits", Mol. Phys. **66**, 1279 - 1289 (1989); doi:10.1080/00268978900100881

[23] V. I. Korobov, private communications (2009, 2011)

[24] T. Schneider, B. Roth, H. Duncker, I. Ernsting and S. Schiller, "All-optical preparation of molecular ions in the rovibrational ground state", Nature Physics **6**, 275-278 (2010); doi:10.1038/nphys1605

[25] D. Bakalov, V. Korobov, S. Schiller, "High-precision calculation of the hyperfine structure of the HD^+ ion", Phys. Rev. Lett. **97**, 243001 (2006); doi:10.1103/PhysRevLett.97.243001

[26] D. Bakalov, V. I. Korobov and S. Schiller, "Magnetic field effects in the transitions of the HD^+ molecular ion and precision spectroscopy", J. Phys. B: At. Mol. Opt. Phys. **44**, 025003 (2011); doi: 10.1088/0953-4075/44/2/025003

[27] P. Blythe, B. Roth, U. Fröhlich, H. Wenz, S. Schiller "Production of cold trapped molecular hydrogen ions", Phys. Rev. Lett. **95**, 183002 (2005); doi:10.1103/PhysRevLett.95.183002

[28] S. Vasilyev, A. Nevsky, I. Ernsting, M. Hansen, J. Shen, and S. Schiller, "Compact all-solid-state continuous-wave single-frequency UV source with frequency stabilization for laser cooling of Be^+ ions", Appl. Phys. B **103**, 27 - 33 (2011); doi: 10.1007/s00340-011-4435-1

[29] S. Schiller, B. Roth, F. Lewen, O. Ricken, M. Wiedner, "Ultra-narrow-linewidth continuous-wave THz sources based on multiplier chains" Appl. Phys. B **95**, 55 - 61 (2009); doi: 10.1007/s00340-008-3279-9

[30] P. Staanum, K. Højbjerre, P. Skyt, A. Hansen and M. Drewsen, "Rotational laser cooling of vibrationally and translationally cold molecular ions", Nature Physics **6**, 271 - 274 (2010); doi:10.1038/nphys1604
[31] see supplemental materials in [24]